

New Physics Models Facing Lepton Flavor Violating Higgs Decays

NEJC KOŠNIK¹

Department of Physics, University of Ljubljana, Jadranska 19, 1000 Ljubljana, Slovenia

and

Jožef Stefan Institute, Jamova 39, P.O. Box 3000, 1001 Ljubljana, Slovenia

We speculate about the possible interpretations of the recently observed excess in the $h \rightarrow \tau\mu$ decay. We derive a robust lower bound on the Higgs boson coupling strength to a tau and a muon, even in presence of the most general new physics affecting other Higgs properties. Then we reevaluate complementary indirect constraints coming from low energy observables as well as from theoretical considerations. In particular, the tentative signal should lead to $\tau \rightarrow \mu\gamma$ at rates which could be observed at Belle II. In turn we show that, barring fine-tuned cancellations, the effect can be accommodated within models with an extended scalar sector. These general conclusions are demonstrated in explicit new physics models. Finally we show how, given the $h \rightarrow \tau\mu$ signal, the current and future searches for $\mu \rightarrow e\gamma$ and $\mu \rightarrow e$ nuclear conversions unambiguously constrain the allowed rates for $h \rightarrow \tau e$.

PRESENTED AT

The 7th International Workshop on Charm Physics
(CHARM 2015)
Detroit, MI, 18-22 May, 2015

¹Supported by Slovenian research agency.

1 Introduction

The discovery of the Higgs boson [1, 2] offers numerous observables where the validity of the Standard Model (SM) can be tested. The CMS collaboration has recently reported a slight excess with a significance of 2.4σ in the search for LFV decay $h \rightarrow \tau\mu$ [3]. The best fit for the branching ratio of the Higgs boson to $\tau\mu$ under assumption of SM Higgs production is found to be

$$\mathcal{B}(h \rightarrow \tau\mu) = (0.84^{+0.39}_{-0.37}) \% . \quad (1)$$

This recent hint has received great attention in the literature (see [4] and references therein). An ATLAS study of $h \rightarrow \tau\mu$ [5] in the hadronic τ channel observes no excess and is consistent with the CMS result (1).

In light of the tentative signal it is instructive to revisit compatibility of such large $\mathcal{B}(h \rightarrow \tau\mu)$ with other low-energy lepton flavor violation (LFV) probes in the context of popular New physics (NP) models.

2 Higgs effective theory approach

The mass terms and Higgs boson couplings of charged leptons after electroweak symmetry breaking (EWSB) can be parametrized in the general case as

$$\mathcal{L}_{Y_\ell}^{\text{eff.}} = -m_i \delta_{ij} \bar{\ell}_L^i \ell_R^j - y_{ij} \left(\bar{\ell}_L^i \ell_R^j \right) h + \dots + \text{h.c.} , \quad (2)$$

where the ellipsis denotes non-renormalizable terms involving more than one Higgs boson. While in the SM the Yukawas $y \sim m$ are diagonal in the mass basis, NP could misalign the two matrices and via $y_{\tau\mu}$ and/or $y_{\mu\tau}$ induce $h \rightarrow \tau\mu$ decays with a branching ratio of $\mathcal{B}(h \rightarrow \tau\mu) = \frac{m_h}{8\pi\Gamma_h} (|y_{\tau\mu}|^2 + |y_{\mu\tau}|^2)$. If one assumes that the total Higgs boson decay width (Γ_h) is SM-like and enlarged only by the contribution from $h \rightarrow \tau\mu$ then the measurement in Eq. (1) can be interpreted as a two-sided bound, $0.0019(0.0008) < \sqrt{|y_{\tau\mu}|^2 + |y_{\mu\tau}|^2} < 0.0032(0.0036)$ at 68% (95%) C.L.. In general, the experimentally measured $h \rightarrow \tau\mu$ branching fraction depends also on other Higgs couplings contributing both to its total decay width (Γ_h) as well as its production cross-section (σ_h). In particular, a given signal can be reproduced for larger (smaller) values of $|y_{\tau\mu}|$ and $|y_{\mu\tau}|$ by enhancing (suppressing) Γ_h and/or suppressing (enhancing) σ_h . Individual effects of Γ_h and σ_h can be disentangled by performing a global fit to all Higgs production and decay event yields at the LHC [4]. Numerically, we find in this case

$$0.0017(0.0007) < \sqrt{|y_{\tau\mu}|^2 + |y_{\mu\tau}|^2} < 0.0036(0.0047) \text{ at 68\% (95\%) C.L.} . \quad (3)$$

In the following we assume the SM contains all the relevant degrees of freedom at energies $\mathcal{O}(\text{few } 100) \text{ GeV}$, whereas for the additional heavy degrees of freedom we

assume they been integrated out. The natural ranges for the effective Higgs couplings follow from the hierarchy between the muon and tau lepton masses [6, 7],

$$\sqrt{|y_{\tau\mu}y_{\mu\tau}|} \lesssim \frac{\sqrt{m_\mu m_\tau}}{v} = 0.0018. \quad (4)$$

It is interesting to note that almost the whole parameter space in allowed by $h \rightarrow \tau\mu$ is also compatible with the above naturalness criterium [4].

Phenomenologically the most relevant low-energy constraints on this scenario are the one- and two-loop contributions to the operators $\bar{L}H(\sigma \cdot B)E$ and $\bar{L}\tau_a H(\sigma \cdot W^a)E$, where $\sigma_{\mu\nu} = i[\gamma_\mu, \gamma_\nu]/2$, $B_{\mu\nu}$ and $W_{\mu\nu}^a$ are the hypercharge and weak isospin field strengths, respectively, and τ_a are the Pauli matrices. These operators can mediate the strongly constrained radiative LFV decays. The most stringent constraint comes from the $\tau \rightarrow \mu\gamma$ decay [8], mediated by the effective Lagrangian

$$\mathcal{L}_{\text{eff.}} = c_L \mathcal{Q}_{L\gamma} + c_R \mathcal{Q}_{R\gamma} + \text{h.c.}, \quad (5)$$

where $\mathcal{Q}_{L,R\gamma} = (e/8\pi^2)m_\tau(\bar{\mu}\sigma^{\alpha\beta}P_{L,R}\tau)F_{\alpha\beta}$, $P_{L,R} = (1 \mp \gamma_5)/2$ and $F_{\alpha\beta}$ is the electromagnetic field strength tensor. The resulting EFT correlation between $\mathcal{B}(h \rightarrow \tau\mu)$ in and $\mathcal{B}(\tau \rightarrow \mu\gamma)$ is shown in left-hand panel in Fig. 1 (diagonal dashed orange line), assuming SM values of all Higgs boson couplings except $y_{\tau\mu}$ and $y_{\mu\tau}$. In the same plot, the CMS preferred range of $\mathcal{B}(h \rightarrow \tau\mu)$ in Eq. (1) is displayed by the horizontal blue band, while the current ($\mathcal{B}(\tau \rightarrow \mu\gamma) < 4.4 \times 10^{-8}$ @ 90% C.L.) [9] and projected future ($\mathcal{B}(\tau \rightarrow \mu\gamma) < 3 \times 10^{-9}$ @ 90% C.L.) [10] indirect constraints are shaded in light and dark gray vertical bands, respectively. We observe that within the EFT approach, the CMS signal is well compatible with the non-observation of $\tau \rightarrow \mu\gamma$ at the B factories and will marginally remain so even at Belle II.

3 Type-III Two Higgs Doublet Model

Extensions of the SM with an additional $SU(2)_L$ doublet scalar are an effective description of several NP scenarios (e.g. supersymmetric extensions or models addressing the strong CP problem via a Peccei-Quinn symmetry), for a recent review c.f. [7]. The most extensively studied version of the Two Higgs Doublet Model (THDM) is the type-II model in which one of the doublets couples to up-type quarks, while the other one couples to down-type quarks and charged leptons, avoiding in this way the tree level flavor changing neutral currents (FCNCs). All LFV in this case comes at 1-loop and is aligned with the SM flavor structure thus rendering LFV processes to a negligible level, compared to the one of the SM [4]. In type-III THDM Yukawa couplings are generic and allow for large LFV. In the case with a MSSM-like Higgs potential the following relations hold [11]

$$\tan \beta = \frac{v_u}{v_d}, \quad \tan 2\alpha = \tan 2\beta \frac{m_A^2 + m_Z^2}{m_A^2 - m_Z^2}, \quad (6)$$

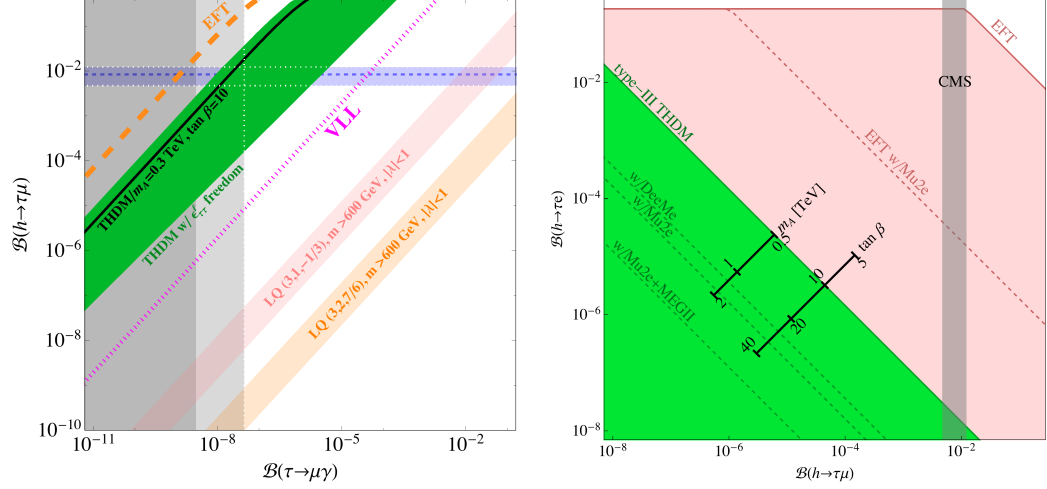


Figure 1: Left-hand side panel: Correlation between $\mathcal{B}(h \rightarrow \tau\mu)$ and $\mathcal{B}(\tau \rightarrow \mu\gamma)$ in various NP scenarios. The present experimental result for $\mathcal{B}(h \rightarrow \tau\mu)$ is shown in horizontal blue band [3]. Current and future projections for $\mathcal{B}(\tau \rightarrow \mu\gamma)$ experimental sensitivity are represented with vertical light [9] and dark [10] gray bands, respectively. Superimposed are the predictions within the EFT approach (diagonal dashed orange line), in the type-III THDM (green and black bands), and in models with scalar leptoquarks (diagonal red and orange shaded band). Right-hand side panel: Allowed region in the $\mathcal{B}(h \rightarrow \tau e)$ – $\mathcal{B}(h \rightarrow \tau\mu)$ plane when experimental upper bounds on $\mu \rightarrow e\gamma$ and $\mu - e$ conversion rates are taken into account. Pink region is permitted in the effective theory setting while the dashed line indicates how much the region will shrink if Mu2e and MEG II experiments see no signal events. Green region is allowed within type-III THDM model with $m_A = 0.5$ TeV and $\tan\beta = 10$. Rulers indicate how much the region shrinks with increasing $\tan\beta$ or m_A , while dashed lines correspond to improved experimental upper bounds on $\mu \rightarrow e\gamma$ and $\mu - e$ as described in the text.

while for the masses $m_{H^\pm}^2 = m_A^2 + m_W^2$ and $m_H^2 = m_A^2 + m_Z^2 - m_h^2$. Here β is the angle that diagonalizes the mass matrices of charged scalars and pseudoscalars while α is an analogous angle for the neutral scalars. The relevant part for the discussion of LFV are the Yukawa couplings in the charged lepton mass eigenstate basis [11]

$$\mathcal{L} = \frac{y_{fi}^{H_k}}{\sqrt{2}} H_k \bar{\ell}_{L,f} \ell_{R,i} + \frac{y_{fi}^{H^+}}{\sqrt{2}} H^+ \bar{\nu}_{L,f} \ell_{R,i} + \text{h.c.}, \quad (7)$$

where the LFV Yukawa couplings can be written as

$$y_{fi}^{H_k} = x_d^k \frac{m_{\ell_i}}{v_d} \delta_{fi} - \epsilon_{fi}^\ell (x_d^k \tan\beta - x_u^{k*}). \quad (8)$$

The off-diagonal parameters ϵ_{fi}^ℓ drive the LFV phenomena, while the coefficients x_q^k for $H_k = (H, h, A)$ can be found in [4]. Using the above relations, we find the tree-level result for the $h \rightarrow \tau\mu$ branching fraction,

$$\mathcal{B}(h \rightarrow \tau\mu) = \frac{m_h}{16\pi\Gamma_h} (\sin\alpha \tan\beta + \cos\alpha)^2 (|\epsilon_{\mu\tau}^\ell|^2 + |\epsilon_{\tau\mu}^\ell|^2) . \quad (9)$$

We have found that even for light pseudoscalar masses (m_A), modifications of hWW and hZZ relative to their SM values is negligible [4].

The decay width of $\tau \rightarrow \mu\gamma$ is driven by a one- and two-loop Barr-Zee diagrams with virtual charged or neutral Higgses. At one-loop the amplitude is suppressed by two small Yukawa couplings, while the two-loop result is proportional to y_{tt} and a single LFV Yukawa. Indeed one finds that Barr-Zee contributions dominate the rate of $\tau \rightarrow \mu\gamma$ [4]. We sample the parameter space of $\epsilon_{\tau\mu}^\ell, \epsilon_{\mu\tau}^\ell, \epsilon_{\tau\tau}^\ell$ for a chosen values of $\tan\beta$ and m_A . The ranges allowed for $\epsilon_{\tau\mu,\mu\tau}^\ell$ are required to fulfill the naturalness criterium of Eq. (4) and stay within the perturbative regime.

The 1-loop amplitude of the $\tau \rightarrow \mu\gamma$ process further depends on the diagonal $y_{\tau\tau}^h$ Yukawa coupling which is experimentally constrained by the searches for $h \rightarrow \tau\tau$ decays by the ATLAS [12] and CMS [13] experiments. The naively averaged signal strength of two $\tau\tau$ signal strengths results in $\mu^{\tau\tau} = 1.02_{-0.20}^{+0.21}$ which directly constrains $y_{\tau\tau}^h$. A scenario with SM-like $y_{\tau\tau}^h$ coupling corresponding to $\mu^{\tau\tau} = 1$ for fixed $\tan\beta = 10$ and $m_A = 0.3$ TeV is presented in left-hand side panel in Fig. 1 by a black narrow stripe. This scenario easily passes both experimental constraints. On the other hand, for masses m_A significantly larger than 500 GeV it is not possible to reconcile both predictions with the corresponding experimental values. Allowing $\epsilon_{\tau\tau}^\ell$ to departure from zero within the allowed range we obtain correlation represented by the green band in left-hand side panel in Fig. 1. In particular, this additional freedom in $\tau \rightarrow \mu\gamma$ breaks the strict correlation with the $h \rightarrow \tau\mu$ rate.

4 Scalar Leptoquarks

A scalar leptoquark state (LQ) can induce $h \rightarrow \tau\mu$ decay via quark-LQ penguin diagrams. Inspection of the helicity structure of the relevant diagrams reveals that both chiralities of leptons and top quark have to couple to the LQ state, in order keep the leptoquark couplings perturbative [4]. LQ state can couple to the Higgs also via the ‘‘Higgs portal’’ operator, $-\lambda H^\dagger H \Delta^\dagger \Delta$ that comes with an additional parameter, λ .

4.1 The $\Delta_1 = (\mathbf{3}, \mathbf{1}, -1/3)$ case

The Yukawa couplings of Δ_1 are given by the following Lagrangian

$$\mathcal{L}_{\Delta_1} = y_{ij}^L \bar{Q}^{i,a} \Delta_1 \epsilon^{ab} L^{Cj,b} + y_{ij}^R \bar{U}^i \Delta_1 E^{Cj} + \text{h.c.} , \quad (10)$$

where $Q^i = (u_L^i, d_L^i)^T$ and $U^i = u_R^i$ are the quark weak doublets and up-quark singlets, respectively. We explicitly show flavor indices $i, j = 1, 2, 3$, and $SU(2)$ indices $a, b = 1, 2$, with $\epsilon_{12} = 1$. The $h \rightarrow \tau\mu$ decay width in the presence of Δ_1 scalar is then,

$$\Gamma(h \rightarrow \tau\mu) = \frac{9m_h m_t^2}{2^{13}\pi^5 v^2} \left(|y_{t\mu}^L y_{t\tau}^R|^2 + |y_{t\tau}^L y_{t\mu}^R|^2 \right) |g_1(\lambda, m_{\Delta_1})|^2. \quad (11)$$

Here the relevant loop function further depends on the portal coupling λ and is given in [4]. The state Δ_1 also contributes to the $\tau \rightarrow \mu\gamma$ via same y couplings as the ones present in $h \rightarrow \tau\mu$:

$$\mathcal{B}(\tau \rightarrow \mu\gamma) = \frac{\alpha m_\tau^3}{2^{12}\pi^4 \Gamma_\tau} \frac{m_t^2}{m_{\Delta_1}^4} h_1(x_t)^2 \left(|y_{t\mu}^L y_{t\tau}^R|^2 + |y_{t\tau}^L y_{t\mu}^R|^2 \right), \quad (12)$$

where $x_t = m_t^2/m_{\Delta_1}^2$ and expression for the h_1 function can be found in Ref. [4].

The impact of a non-zero Higgs portal coupling λ in the scenario with Δ_1 has also been studied. As an example, for $m_{\Delta_1} = 650 \text{ GeV}$ the loop function dependence on the portal coupling is $g_1 = -(0.26 + 0.12\lambda)$. Thus, a positive large λ could relax the leptoquark Yukawa couplings and yield sizable $h \rightarrow \tau\mu$ rates without violating the $\tau \rightarrow \mu\gamma$ constraint. However, the Higgs portal coupling also induces corrections to the $h \rightarrow \gamma\gamma$ decay and to gluon-gluon fusion (ggF) induced Higgs production with the leptoquark running in the triangular loop. Taking those modifications of the Higgs couplings into account we have found that one can compensate small leptoquark Yukawas by scaling up λ , which is itself bounded from above only by perturbativity requirements [4].

The correlation between the $h \rightarrow \tau\mu$ and $\tau \rightarrow \mu\gamma$ branching ratios in presence of the $(3, 1, -1/3)$ leptoquark state for $|\lambda| < 1$ and $m_{\Delta_1} > 600 \text{ GeV}$ is depicted in left-hand side panel in Fig. 1 with a pink stripe, demonstrating that $\tau \rightarrow \mu\gamma$ basically excludes this LQ state as an explanation of $h \rightarrow \tau\mu$ signal.

4.2 The $\Delta_2 = (3, 2, 7/6)$ case

The Yukawa couplings of the Δ_2 leptoquark to SM fermions are

$$\mathcal{L}_{\Delta_2} = y_{ij}^L \bar{E}^i \Delta_2^{a*} Q^{j,a} - y_{ij}^R \bar{U}^i \Delta_2^a \epsilon^{ab} L^{j,b} + \text{h.c.}, \quad (13)$$

The $h \rightarrow \tau\mu$ decay rate in this case is

$$\Gamma(h \rightarrow \tau\mu) = \frac{9m_h m_t^2}{2^{13}\pi^5 v^2} |g_1(\lambda, m_{\Delta_2})|^2 \left(|y_{t\mu}^L y_{t\tau}^R|^2 + |y_{t\tau}^L y_{t\mu}^R|^2 \right). \quad (14)$$

Allowed values for the Higgs portal coupling λ can be inferred from a global fit to the Higgs data as has been done for the portal coupling of the $(3, 1, -1/3)$ state.

The decay width of $\tau \rightarrow \mu\gamma$ are proportional to the couplings responsible for $h \rightarrow \tau\mu$:

$$\mathcal{B}(\tau \rightarrow \mu\gamma) = \frac{\alpha m_\tau^3}{2^{12} \pi^4 \Gamma_\tau} \frac{m_t^2}{m_\Delta^4} h_2(x_t)^2 (|y_{t\tau}^R y_{\mu t}^L|^2 + |y_{t\mu}^R y_{\tau t}^L|^2). \quad (15)$$

In this leptoquark scenario the bound on $\mathcal{B}(\tau \rightarrow \mu\gamma)$ excludes sizable $\mathcal{B}(h \rightarrow \tau\mu)$ due to the strict correlation between the two observables. See the orange stripe in left-hand side panel in Fig. 1, where the portal coupling is restricted to $|\lambda| < 1$.

5 $h \rightarrow \tau\mu$ vs. $h \rightarrow \tau e$

A positive indication for $h \rightarrow \tau\mu$ decay can be combined with stringent experimental limits on $\mu-e$ LFV processes to constrain $\tau-e$ processes. In particular, in models with tree-level $h \rightarrow \tau\mu$ (EFT, THDM III) the product of the $\mathcal{B}(h \rightarrow \tau e)$ and $\mathcal{B}(h \rightarrow \tau\mu)$ is bounded from above by the rates of $\mu \rightarrow e\gamma$ and $\mu-e$ conversion on nuclei. This is due to the fact that tree level Higgs decays to $\tau\mu$ (τe) depend on $y_{\mu\tau, \tau\mu}$ ($y_{e\tau, \tau e}$) while the same sets of couplings contribute at the loop level to $\mu \rightarrow e\gamma$ and $\mu-e$ conversion via diagrams with a virtual τ . In the effective theory framework, the contributions to the $\mu \rightarrow e\gamma$ process stemming from a virtual τ are m_τ enhanced with respect to diagrams with intermediate μ or e states [8] leading to

$$c_L^\tau \simeq \frac{m_\tau}{m_\mu} \frac{-3 + 4x_\tau - x_\tau^2 - 2 \log x_\tau}{8m_h^2(1-x_\tau)^3} y_{\mu\tau}^* y_{\tau e}^*, \quad x_\tau = \frac{m_\tau^2}{m_h^2}, \quad (16)$$

where we have neglected the effects of the light lepton masses. The coefficient c_R^τ is obtained from Eq. (16) by replacing $y_{ij} \rightarrow y_{ji}^*$. The $\mu \rightarrow e\gamma$ branching fraction is thus sensitive to a distinct combination of the LFV Yukawas:

$$\mathcal{B}(\mu \rightarrow e\gamma) \simeq \mathcal{B}_0^{\mu \rightarrow e\gamma} (|y_{\mu\tau} y_{\tau e}|^2 + |y_{\tau\mu} y_{e\tau}|^2), \quad \mathcal{B}_0^{\mu \rightarrow e\gamma} = 185. \quad (17)$$

On the other hand, $\mu-e$ conversion on nuclei is most sensitive to vector current effective operators $(\bar{e}\gamma_\nu P_{L,R}\mu)(\bar{q}\gamma^\nu q)$. The branching fraction $\mathcal{B}(\mu \rightarrow e)_{\text{Au}} \equiv \Gamma(\mu \rightarrow e)_{\text{Au}}/\Gamma_{\text{capture Au}}$ can be put in the form

$$\mathcal{B}(\mu \rightarrow e)_{\text{Au}} = \mathcal{B}_0^{\mu e} (|y_{e\tau} y_{\mu\tau}|^2 + |y_{\tau e} y_{\tau\mu}|^2), \quad \mathcal{B}_0^{\mu e} = 4.67 \times 10^{-4}, \quad (18)$$

where the relevant numerics have been taken from Ref. [14] (also c.f. [4]). The complementary information on the LFV couplings extracted from $\mu \rightarrow e\gamma$ and $\mu-e$ conversion allows for correlation between the Higgs LFV $h \rightarrow \tau\mu$ and $h \rightarrow \tau e$ decays:

$$\mathcal{B}(h \rightarrow \tau\mu)\mathcal{B}(h \rightarrow \tau e) = 8 \times 10^{-10} \left[\frac{\mathcal{B}(\mu \rightarrow e\gamma)}{10^{-13}} \right] + 3 \times 10^{-4} \left[\frac{\mathcal{B}(\mu \rightarrow e)_{\text{Au}}}{10^{-13}} \right]. \quad (19)$$

The best experimental limit on $\mathcal{B}(\mu \rightarrow e)_{\text{Au}} < 7 \times 10^{-13}$ (at 90% C.L.) was achieved by the SINDRUM II Collaboration [15] while the best upper bound on $\mathcal{B}(\mu \rightarrow e\gamma) < 5.7 \times 10^{-13}$ (at 90% C.L.) was recently determined by the MEG Collaboration [16]. Note that with the current experimental data the sum on the right-hand side of Eq. (19) is completely saturated by the $\mu - e$ conversion contribution. Combining the two bounds with the central value for the $h \rightarrow \tau\mu$ branching fraction in Eq. (1) leads to an upper bound $\mathcal{B}(h \rightarrow \tau e) < 0.26$. This is above the current indirect constraint coming from searches for $\tau \rightarrow e\gamma$ [9] which reads $\mathcal{B}(h \rightarrow \tau e) < 0.19$. Future improvements of bounds on $\mu \rightarrow e\gamma$ and especially $\mu - e$, and assuming $\mathcal{B}(h \rightarrow \tau\mu)$ stays at the percent level, will indirectly probe $\mathcal{B}(h \rightarrow \tau e)$ at the 10^{-5} level [4]. Similar analysis can be carried over to the THDM III framework, where the resulting bound on $h \rightarrow \tau e$ renders this decay invisible at the LHC (green region in right-hand side panel in Fig. 1).

6 Conclusions

Motivated by the experimental indication of $h \rightarrow \tau\mu$ events by the CMS Collaboration we have examined the implications of LFV Higgs decays at the percent level on several extensions of the SM. We have shown how a tentative $\mathcal{B}(h \rightarrow \tau\mu)$ signal can be combined with other Higgs measurements to yield a robust lower bound on the effective LFV Higgs Yukawa couplings to taus and muons. In explicit NP models, the $\tau \rightarrow \mu\gamma$ constraint is generically more severe. In fact, an eventual observation of $h \rightarrow \tau\mu$ at the LHC together with indirect constraints would point in the direction of an extended SM scalar sector, minimal example being THDM of type III. We have also examined models where $h \rightarrow \tau\mu$ is generated at loop level to demonstrate difficulties with these models. Finally, we have combined the signal of $h \rightarrow \tau\mu$ with experimental limits on $\mu \rightarrow e\gamma$ decays and $\mu - e$ conversions in nuclei to yield robust bounds on $\mathcal{B}(h \rightarrow \tau e)$. In particular, considering only the Higgs EFT effects, the two LFV Higgs decay rates could still be comparable. On the other hand, the THDM III cannot accommodate both branching ratios at the percent level. It turns out that currently planned improvements in experimental searches for $\mu - e$ LFV processes will be able to probe the product $\mathcal{B}(h \rightarrow \tau\mu)\mathcal{B}(h \rightarrow \tau e)$ at the 10^{-7} level in generic EFT and to order 10^{-12} or better within the THDM III.

References

- [1] Georges Aad et al. *Phys.Lett.* B716 (2012). arXiv:1207.7214 [hep-ex].
- [2] Serguei Chatrchyan et al. *Phys.Lett.* B716 (2012). arXiv:1207.7235 [hep-ex].
- [3] Vardan Khachatryan et al. (2015). arXiv:1502.07400 [hep-ex].

- [4] Ilja Doršner et al. *JHEP* 06 (2015). arXiv:1502.07784 [hep-ph].
- [5] Georges Aad et al. (2015). arXiv:1508.03372 [hep-ex].
- [6] T.P. Cheng and Marc Sher. *Phys.Rev.* D35 (1987).
- [7] G.C. Branco et al. *Phys.Rept.* 516 (2012). arXiv:1106.0034 [hep-ph].
- [8] Roni Harnik, Joachim Kopp, and Jure Zupan. *JHEP* 1303 (2013). arXiv:1209.1397 [hep-ph].
- [9] Bernard Aubert et al. *Phys.Rev.Lett.* 104 (2010). arXiv:0908.2381 [hep-ex].
- [10] T. Aushev et al. (2010). arXiv:1002.5012 [hep-ex].
- [11] Andreas Crivellin, Ahmet Kokulu, and Christoph Greub. *Phys.Rev.* D87.9 (2013). arXiv:1303.5877 [hep-ph].
- [12] Georges Aad et al. (2015). arXiv:1501.04943 [hep-ex].
- [13] Serguei Chatrchyan et al. *JHEP* 1405 (2014). arXiv:1401.5041 [hep-ex].
- [14] Ryuichiro Kitano, Masafumi Koike, and Yasuhiro Okada. *Phys.Rev.* D66 (2002). arXiv:hep-ph/0203110 [hep-ph].
- [15] Wilhelm H. Bertl et al. *Eur.Phys.J.* C47 (2006).
- [16] J. Adam et al. *Phys.Rev.Lett.* 110 (2013). arXiv:1303.0754 [hep-ex].